

CAPILLARY PRESSURE AND PHONONS IN Ag, Au, Cu AND Ni NANOPARTICLES

R. MEYER^{a*}, S. PRAKASH^b, and P. ENTEL^c

^a*Département de Physique, Université de Montréal,
C.P. 6128 succ. centre-ville, Montréal (Québec) H3C 3J7, Canada*

^b*Department of Physics, Panjab University, Chandigarh 160014, India*

^c*Theoretische Tieftemperaturphysik,
Gerhard-Mercator-Universität Lotharstraße 1, 47048 Duisburg, Germany*

(Received ...)

Abstract

Spherical nanoparticles of fcc metals with diameters between 2 and 10 nm have been studied by molecular-dynamics simulations. The results show that despite of the small size of the clusters the Kelvin-equation accounts for the capillary pressure building up in the particles. Furthermore, the simulations show that the capillary pressure leads to a shift of the local vibrational density of states in the core of the particles to higher energies. The cluster's total vibrational density of states is found to be broadened by the contributions from surface atoms. The connection between this broadening and the density of states in nanocrystalline materials is discussed.

Keywords: Capillary pressure, Molecular-dynamics simulations, Phonon density of states

1. INTRODUCTION

In recent years, clusters containing 10^2 to 10^5 atoms have attracted a great deal of attention by materials scientists – see e.g. *Science* **271**, no. 5271 (1996). Due to their high surface to volume ratio and their small size in the

*Corresponding author, tel. +1-514-343-6734, fax: +1-514-343-2071 email: meyer@magellan.umontreal.ca

range of nanometers these clusters have distinctly different physical properties than the corresponding bulk systems. This is of high technological interest since consolidation of such clusters to so-called cluster-assembled materials might enable the fabrication of materials with specifically tailored properties.

In this work we study the capillary pressure inside spherical metallic fcc nanoparticles. Capillary pressure is a pressure acting inside a system which is caused by a curvature of its surface. For a macroscopic spherically shaped body the magnitude of the capillary pressure p is given by the generalized Kelvin equation

$$p = \frac{2 \tau}{R}, \quad (1)$$

where R is the radius of the particle and τ is the surface stress. While in the case of a liquid, the surface stress τ is isotropic and equal to the surface tension of the material, the situation is more complicated for crystalline solids. In this case the surface stress becomes anisotropic and it is no longer equal to the surface tension (Nozières and Wolf, 1988; Wolf and Nozières, 1988; Sanfeld and Steinchen, 2000). The value of τ in Eq. (1) for a solid is therefore not directly related to the surface energy of the system and it has to be understood as an average over all the different crystalline facets composing the surface of the sphere.

For nanoclusters, the applicability of Eq. (1) is not directly clear since the thermodynamic arguments on which this equation is based – see e.g. Sanfeld and Steinchen (2000) – do not necessarily hold for a system, where the number of particles located at the surface is comparable to the total number of particles. In addition to this, increasing deviations from an ideal spherical shape of the particles might lead to strong fluctuations of the average surface stress τ . In their molecular-dynamics simulation study (Swaminarayan, Najafabadi and Srolovitz, 1994), have found that for nanometer sized, spherical crystallites of fcc metals Eq. (1) remains valid. Nevertheless, it seems to be worth to revisit this question, employing a different parameterization of the interatomic potentials, in order to check whether this result depends on the details of the model used in the simulations. This is the subject of the first part of this work.

The importance of capillary pressure for nanoparticles lies in the inverse dependency of the pressure on the system size as shown by Eq. (1). For typical values of the surface stress the pressure inside nanoparticles eventually reaches the order of GPa and thereby has a strong influence on the properties of the material. This can be seen from the experimentally observed (Mays, Vermaak and Kuhlmann-Wilsdorf, 1968; Wasserman and Vermaak, 1970, 1972; Apai, Hamilton, Stohr and Thomson, 1979; Solliard and Flueli, 1985; Montano, Shenoy, Alp, Schulze *et al.*, 1986) and theoretically calculated (Kara and Rahman, 1998) self-compression of nanoclusters, exemplified by the radial distribution functions given in Fig. 1. In the second part of this work we study the influence of capillary pressure on the vibrational density

of states (DOS) of nanoclusters.

2. COMPUTATIONAL METHODS

We have performed molecular-dynamics simulations of spherical Ag, Au, Cu, and Ni nanoparticles employing interatomic potentials based upon the embedded-atom method (EAM) introduced by Daw and Baskes (1984). The starting configurations were spherical regions cut out of a regular fcc lattice with diameters in the range 2 – 10 nm. The equations of motion of these configurations were integrated at $T = 300$ K in the microcanonical ensemble using the Verlet-Algorithm with a time step of 1.5 fs.

The distribution of stress inside the simulated nanoparticles was calculated with the help of the instantaneous stress tensor

$$\sigma_i^{\alpha\beta} = \frac{1}{\Omega_i} \left(m_i v_i^\alpha v_i^\beta + \sum_{j \neq i} F_{ij}^\alpha r_{ij}^\beta \right). \quad (2)$$

Herein, m_i denotes the mass of atom i and Ω_i its atomic volume. Further, v_i^α , F_{ij}^α , r_{ij}^α are the Cartesian components ($\alpha = x, y, z$) of the atom's velocity, the force between atom i and j , and their distance vector, respectively. From the first invariant of the instantaneous stress tensor defined by Eq. (2) the local pressure $p_i = \frac{1}{3} \text{Tr} \sigma$ can be obtained, while the second invariant $J_i = \frac{1}{2} [\text{Tr}(\sigma_i^T \sigma_i) - 3p_i^2]$ is related to the energy stored in shear stress (Landman, Luedtke and Ringer, 1992). In the application of Eq. (2) attention has to be paid to the calculation of the atomic volume Ω_i . A rigorous calculation of this quantity for all atoms at each time-step is too time-consuming (and probably impossible for surface atoms). Therefore, we actually calculate the averages $\langle p_i \Omega_i \rangle$, $\langle J_i \Omega_i^2 \rangle$ and divide later by the mean atomic volume $\langle \Omega_i \rangle$ of the atoms in the inner part of the clusters (see below).

In addition to the stress distribution we derived the vibrational DOS of the clusters from our simulations. In order to do so, we made use of the fact that for a classical system the vibrational DOS is directly proportional to the temporal Fourier-transform of the velocity autocorrelation function (Lovesey, 1986) which can easily be calculated from the particle trajectories during the simulations.

3. RESULTS

3.1. Capillary Pressure

In Fig. 2 we present as an example the variation of the local stress quantities $\langle p_i \rangle$ and $\langle J_i \Omega_i^2 \rangle$ inside a Ag_{3043} cluster. The upper panel of this figure shows the occurrence of three distinct pressure regimes inside the particle. At the surface the pressure is apparently negative, reflecting the fact that

the system tries to reduce its surface area. Directly below the surface the pressure changes its sign abruptly. The excessive pressure in this region is a consequence of the relaxation of surface atoms and occurs similarly at flat surfaces. Finally, deep in the cluster, the pressure takes a constant value, modified by relaxation modulations. Similar structures have been observed in all of our simulations.

From the lower panel in Fig. 2 it can be seen that the second invariant of the stress tensor has a constant value inside the cluster while it increases considerably at the surface. The value we find inside the cluster agrees well with simulations of bulk silver under the pressure acting inside the particle (1.2 GPa, cf. upper panel of Fig. 2). From this we conclude that the constant value of $\langle J_i \Omega^2 \rangle$ inside the particle results from a regular fcc lattice in this region, whereas the increase of $\langle J_i \Omega^2 \rangle$ near the surface is caused by the asymmetric environment of the outer atoms. The onset of the increase of $\langle J_i \Omega^2 \rangle$ provides a convenient way of defining a core radius r_c inside which a homogeneous bulk structure can be assumed. Moreover, we have used the nearest neighbor distance of the fcc structure inside r_c to calculate the mean atomic volume Ω_i .

Figure 3 shows the variation of the pressure acting on the particle cores as a function of the inverse particle radius R . For our purposes, we defined the particle radius R (which should not be confused with the core radius r_c introduced in the preceding paragraph) as the maximum distance of an atom with a coordination number of at least eight from the particle's center of mass. The linear dependence of the pressure from the cluster radius reveals in accordance with Swaminarayan *et al.* (1994) that over the whole range of sizes Eq. (1) gives a valid description of the pressure inside the simulated particles. The values of the surface stress τ_{sim} resulting from the slopes of the lines in Fig. 3 are given in Table 1 together with the surface energies derived from the excess potential energy of the biggest particles. Although far from being perfect, the agreement between the surface stress data and its experimental counterparts in Table 1 is satisfactory, if one takes into account the high experimental uncertainty and sparse availability of surface stress data. In contrast to this, the surface energies of the simulated clusters are 15 – 25 % smaller than the values determined by Tyson and Miller (1977) from experimental data. This systematic deviation is not specific to our work but a generally observed problem of EAM potentials.

3.2. Phonon Density of States

The presence of high capillary pressures inside the particles as well as the large number of surface atoms has a strong effect on the cluster's vibrational DOS. In order to study this influence, we have calculated the vibrational density of states of a Ag_{531} cluster as well as bulk Ag under pressures of zero and 2.0 GPa, where the latter pressure corresponds to the capillary pressure acting on the cluster's core. The results of these calculations are given in

Fig. 4. All curves have been broadened by a finite linewidth of 0.25 THz in order to reduce the noise.

As one can see from Fig. 4, the cluster's DOS is mostly determined by the contribution of the surface atoms. This is a consequence of the high surface to volume ratio of the particle which means in this case that there are only 87 atoms within the core radius r_c while the surface is made up of 444 atoms. Although the contribution of the core atoms to the total DOS is small, the DOS in the core shows directly the influence of capillary pressure. This can be seen from the fact that the local DOS of the core atoms shown in Fig. 4 perfectly coincides with the bulk result at 2.0 GPa, whereas it is significantly shifted with respect to bulk Ag at 0.0 GPa. This shift is in agreement with the findings of Kara and Rahman (1998).

In contrast to the core atoms which except for the pressure-induced shift show a similar behavior as the bulk, the surface atoms broaden the DOS of the cluster, leading to an enhanced DOS at low and high frequencies. At low energies a similar effect has been observed in many studies of nanocrystalline materials, see e.g. Wolf *et al.* (1995); Trampenau *et al.* (1995); Fultz *et al.* (1997); Frase *et al.* (1997, 1998); Stuhr *et al.* (1998). However, the enhancement of the DOS at low frequencies in nanocrystalline materials is generally much more pronounced than the small increase visible in Fig. 4. In particular (and in contrast to the results of Kara and Rahman (1998)), we do not find a linear behavior of the DOS at vanishing frequencies as seen by Stuhr *et al.* (1998). On the other hand, this is not surprising since a cluster, being a finite system, must have a gap in the spectrum at low frequencies. The existence of this gap is confirmed by a direct diagonalization of the cluster's dynamical matrix which gives a frequency of 0.75 THz for the lowest nonvanishing mode. This result agrees reasonably well with the first peak of the cluster's DOS in Fig. 4. The rather small DOS shown in the figure at lower frequencies is a result of anharmonic effects, the applied 0.25 THz line broadening, and finite simulation time. Note that the DOS of the bulk systems in Fig. 4 is also very low at low energies. This is due to the fact that the bulk results were derived from simulations of finite systems containing $10 \times 10 \times 10$ fcc cells (4000 atoms).

At high phonon frequencies we find a much stronger increase of the DOS in the cluster than in the low frequency regime. The long tail at frequencies above 7 THz is mainly due to the surface atoms. A similar tail has been observed by Fultz *et al.* (1997) and Frase *et al.* (1998), where it has been attributed to large anharmonic damping. In our case, however, the direct diagonalization of the cluster's dynamical matrix reveals the presence of harmonic modes with unusual high frequencies up to 11.7 THz. These modes account at least partially for the high frequency tail of the DOS in our simulations.

4. SUMMARY AND DISCUSSION

In summary, we have done molecular-dynamics simulations of nanometer sized Ag, Au, Cu, and Ni clusters. These simulations show in agreement with the work of Swaminarayan *et al.* (1994), that the Kelvin-equation accounts for the capillary pressure inside such particles. This is not a trivial result. Preliminary results show that if we use a Lennard-Jones potential for the calculation of the interatomic forces, we do not find a linear variation of the pressure inside the particles with the inverse radius. Nevertheless, even in this case a positive pressure is present inside the particles. This proves that the pressure inside the particles has to be attributed to capillary pressure and not to the inward relaxation of surface atoms (only present in the EAM model) as it has been done by Kara and Rahman (1998).

Calculations of the local vibrational DOS inside a Ag_{531} cluster show a shift of the DOS to higher energies compared to bulk Ag without pressure. This shift is perfectly explained by the presence of the capillary pressure as can be seen from our simulations of bulk Ag under pressure. The total vibrational DOS of the particle is significantly broadened due to the surface atoms. This broadening is similar to the observations in nanocrystalline materials. However, the increase of the DOS at low frequencies in our simulations is much smaller than the effect observed in nanocrystalline materials. This can be explained by the limited spatial extent of the cluster which suppresses the existence of long wavelength modes. Finally, the direct diagonalization of the particle's dynamical matrix shows the existence of harmonic modes at much higher frequencies than those occurring in the bulk system. This raises the question whether similar (probably highly localized) modes can, at least partially, account for the high frequency tail in the DOS of nanocrystalline materials.

Acknowledgements

R. M. wishes to thank Prof. L. J. Lewis for many discussions and a critical review of the manuscript of this article. This work has been supported by the Deutsche Forschungsgemeinschaft through Sonderforschungsbereich 445 *Nanoparticles from the Vapor Phase: Synthesis, Characterization, Properties*.

References

- Apai, G., J. F. Hamilton, J. Stohr and A. Thomson (1979). Extended X-ray-absorption fine structure of small Cu and Ni clusters: Binding energy and bond-length changes with cluster size. *Phys. Rev. Lett.*, **43**, 165.
- Daw, M. S. and M. I. Baskes (1984). Embedded-atom method: Derivation and application to impurities, surfaces and other defects in metals. *Phys. Rev. B*, **29**, 6443.

- Frase, H., B. Fultz and J. L. Robertson (1998). Phonons in nanocrystalline Ni₃Fe. *Phys. Rev. B*, **57**, 898.
- Frase, H. N., L. J. Nagel, J. L. Robertson and B. Fultz (1997). Vibrational density of states of nanocrystalline Ni₃Fe. *Phil. Mag. B*, **75**, 335.
- Fultz, B., C. C. Ahn, E. E. Alp, W. Sturhahn *et al.* (1997). Phonons in nanocrystalline ⁵⁷Fe. *Phys. Rev. Lett.*, **79**, 937.
- Kara, A. and T. S. Rahman (1998). Vibrational properties of metallic nanocrystals. *Phys. Rev. Lett.*, **81**, 1453.
- Landman, U., W. D. Luedtke and E. M. Ringer (1992). Atomistic mechanisms of adhesive contact formation and interfacial processes. *Wear*, **153**, 3.
- Lovesey, S. W. (1986). *Condensed matter physics: dynamic correlations*, volume 61 of *Frontiers in Physics*. Benjamin/Cummings, Menlo Park, Calif., 2nd edition.
- Mays, C. W., J. S. Vermaak and D. Kuhlmann-Wilsdorf (1968). On surface stress and surface tension. I. Determination of the surface stress of gold. *Surf. Sci.*, **12**, 134.
- Montano, P. A., G. K. Shenoy, E. E. Alp, W. Schulze *et al.* (1986). Structure of copper microclusters isolated in solid argon. *Phys. Rev. Lett.*, **56**, 2076.
- Nozières, P. and D. E. Wolf (1988). Interfacial properties of elastically strained materials – I. Thermodynamics of a planar interface. *Z. Phys. B*, **70**, 399.
- Sanfeld, A. and A. Steinchen (2000). Surface energy, stress, capillary-elastic pressure and chemical equilibrium constant in nanoparticles. *Surf. Sci.*, **463**, 157.
- Science **271**, no. 5271 (1996). Special issue on nanoparticles, ed. by J. I. Brauman.
- Solliard, C. and M. Flueli (1985). Surface stress and size effect on the lattice parameter in small particles of gold and platinum. *Surf. Sci.*, **156**, 487.
- Stuhr, U., H. Wipf, K. H. Andersen and H. Hahn (1998). Low-frequency modes in nanocrystalline Pd. *Phys. Rev. Lett.*, **81**, 1449.
- Swaminarayan, S., R. Najafabadi and D. J. Srolovitz (1994). Polycrystalline surface properties from spherical crystallites: Ag, Au, Cu and Pt. *Surf. Sci.*, **306**, 367.
- Trampenau, J., K. Bauszus, W. Petry and U. Herr (1995). Vibrational behaviour of nanocrystalline Ni. *Nanostruct. Mater.*, **6**, 551.
- Tyson, W. R. and W. A. Miller (1977). Surface free energies of solid metals: Estimation from liquid surface tension measurements. *Surf. Sci.*, **62**, 267.
- Wasserman, H. J. and J. S. Vermaak (1970). On the determination of a lattice contraction in very small silver particles. *Surf. Sci.*, **22**, 164.

- Wasserman, H. J. and J. S. Vermaak (1972). On the determination of the surface stress of copper and platinum. *Surf. Sci.*, **32**, 168.
- Wolf, D., J. Wang, S. R. Phillpot and H. Gleiter (1995). Phonon-induced anomalous specific heat of a nanocrystalline material by computer simulation. *Phys. Rev. Lett.*, **74**, 4686.
- Wolf, D. E. and P. Nozières (1988). Interfacial properties of elastically strained materials – II. Mechanical and melting equilibrium of a curved interface. *Z. Phys. B*, **70**, 507.

Table 1: Values of surface stress τ_{sim} and surface energy γ_{sim} derived from simulations of nanoclusters at $T = 300$ K in comparison to corresponding experimental values τ_{exp} and γ_{exp} .

	Ag	Au	Cu	Ni
τ_{sim} (N/m)	1.22	1.80	1.70	2.33
τ_{exp} (N/m)	1.42 ^a	1.18 ^b – 3.19 ^c	0.00 ^d	
γ_{sim} (J/m ²)	1.02	1.12	1.52	1.86
γ_{exp} (J/m ²)	1.24 ^e	1.50 ^e	1.78 ^e	2.37 ^e

^aWasserman and Vermaak (1970)

^bMays *et al.* (1968)

^cSolliard and Flueli (1985)

^dWasserman and Vermaak (1972)

^eTyson and Miller (1977)

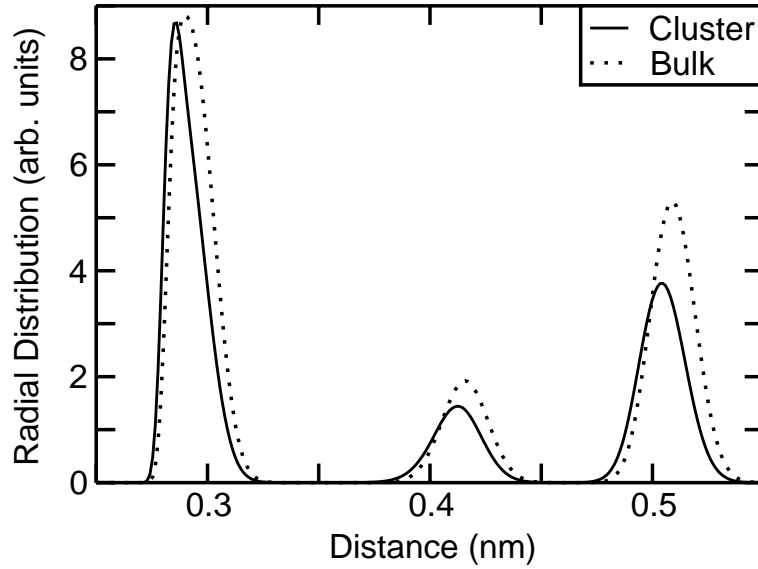


Figure 1: Radial distribution functions of an fcc Ag_{531} cluster and bulk Ag at $T = 300$ K.

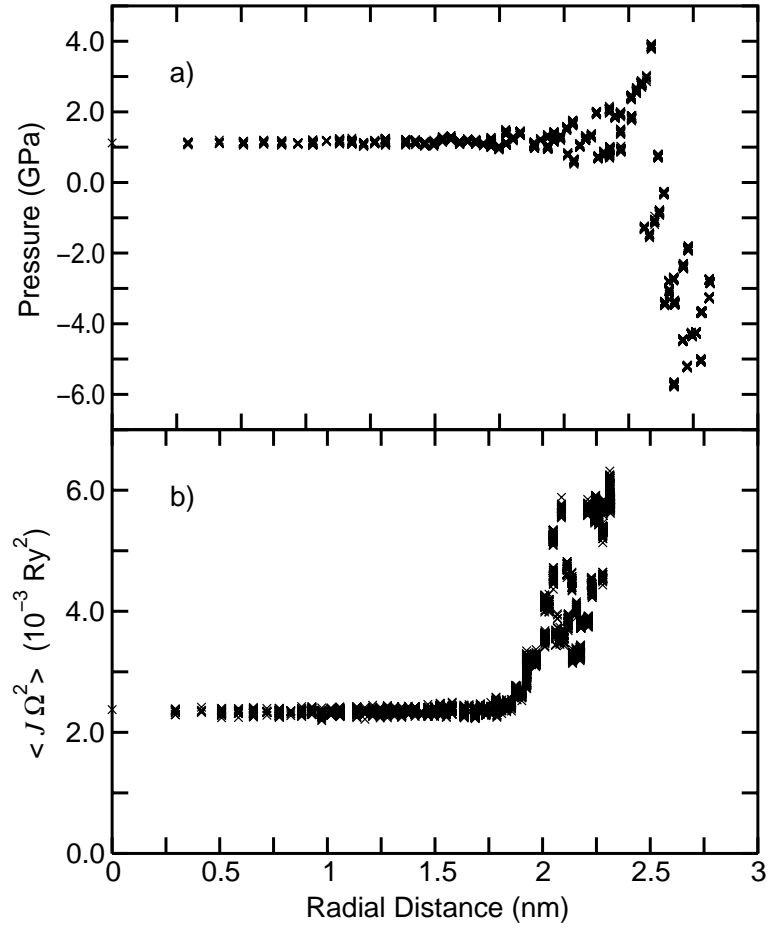


Figure 2: Variations of local stress quantities inside a Ag_{3043} cluster as a function of the distance of the mean atomic position from the cluster's center of mass. Upper panel: pressure $\langle p_i \rangle$, lower panel: $\langle J_i \Omega^2 \rangle$.

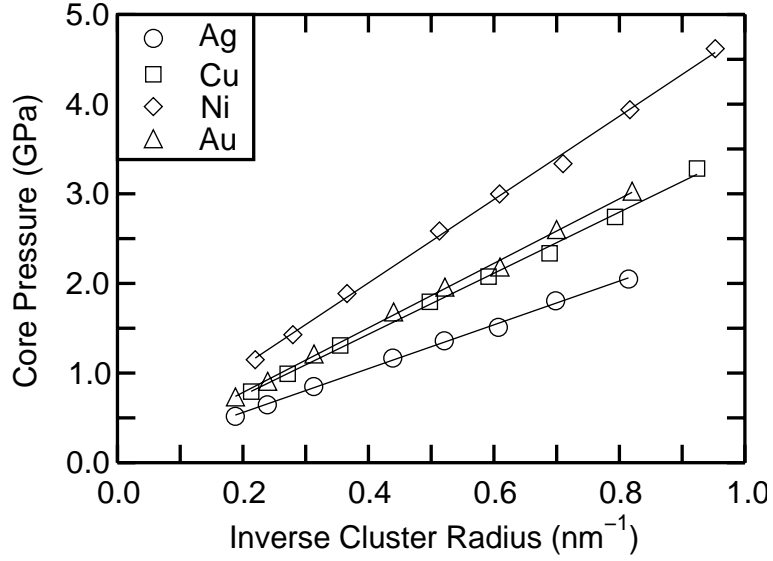


Figure 3: Pressure acting on the cluster cores as a function of the inverse radius of the clusters R^{-1} . The lines represent linear fits to the simulation data.

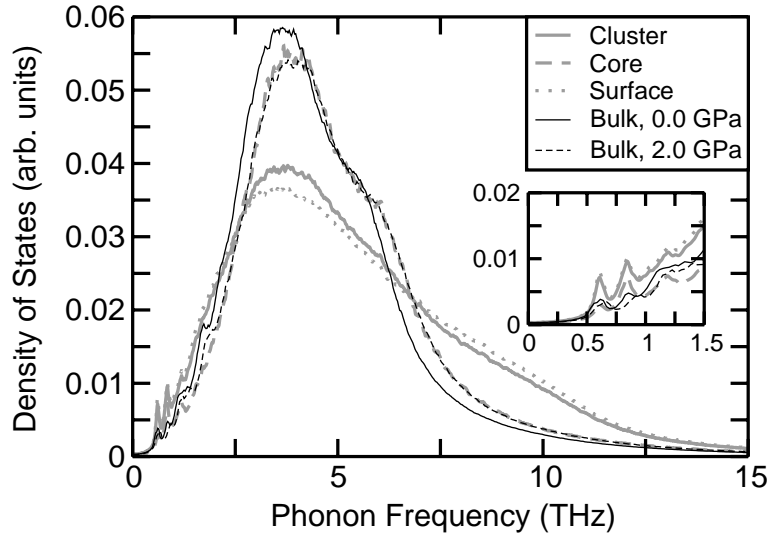


Figure 4: Phonon density of states of a 531 atom Ag cluster (thick solid line), bulk Ag at 0.0 GPa (thin solid line), and bulk Ag at 2.0 GPa (thin dashed line). The dotted and dashed thick lines denote contributions to the cluster DOS coming from atoms inside and outside the core radius r_c , respectively.